JACS JOURNAL OF THE AMERICAN CHEMICAL SOCIETY

Article

Cite This: J. Am. Chem. Soc. 2019, 141, 11036−11049

pubs.acs.org/JACS

Human *NEIL3* Gene Expression Regulated by Epigenetic-Like Oxidative DNA Modification

Aaron M. Fleming,* Judy Zhu, Shereen A. Howpay Manage, and Cynthia J. Burrows*

Department of Chemistry, University of Utah, Salt Lake City, Utah 84112-0850, United States

Supporting Information

ABSTRACT: The *NEIL3* DNA repair gene is induced in cells or animal models experiencing oxidative or inflammatory stress along with oxidation of guanine (G) to 8-oxo-7,8-dihydroguanine (OG) in the genome. We hypothesize that a G-rich promoter element that is a potential G-quadruplex-forming sequence (PQS) in *NEIL3* is a site for introduction of OG with epigenetic-like potential for gene regulation. Activation occurs when OG is formed in the *NEIL3* PQS located near the transcription start site. Oxidative stress either introduced by TNFα or synthetically incorporated into precise locations focuses the base excision repair process to read and catalyze removal of OG via OG-glycosylase I (OGG1), yielding an abasic site (AP). Thermodynamic studies showed that AP destabilizes the duplex, enabling a structural transition of the sequence to a G-quadruplex (G4) fold that positions the AP in a loop facilitated by the *NEIL3* PQS having five G runs in which the four unmodified runs adopt a stable G4. This presents AP to apurinic/apyrimidinic endonuclease 1 (APE1) that poorly cleaves the AP backbone in this context according to in vitro studies, allowing the protein to function as a trans activator of transcription. The proposal is supported by chemical studies in cellulo and in vitro. Activation of *NEIL3* expression via the proposed mechanism allows cells to respond to mutagenic DNA damage removed by NEIL3 associated with oxidative or inflammatory stress. Lastly, inspection of many mammalian genomes identified conservation of the *NEIL3* PQS, suggesting this sequence was favorably selected to function as a redox switch with OG as the epigenetic-like regulatory modification.

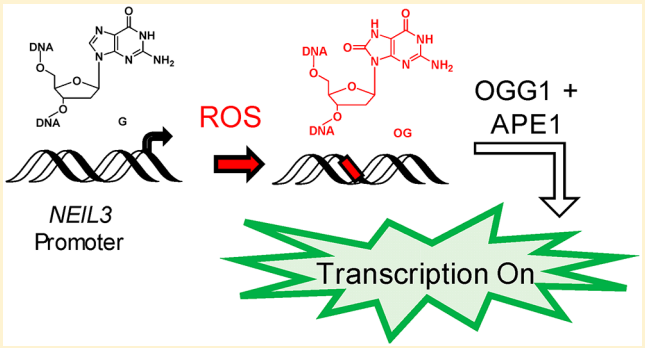

INTRODUCTION

The levels of reactive oxygen and nitrogen species (ROS and RNS) such as $O_2^{\bullet-}$, H_2O_2, $HO^{\bullet}$, NO, and $ONOO^-$ increase in cells under oxidative stress and inflammation.[1,2] These reactive species can readily oxidize many cellular components, while oxidation of DNA can be most profound in the long term.[3,4] Oxidized DNA bases can result in mutations to the genome in the absence of faithful DNA repair that are passed on to future generations.[5,6] In nucleic acids, the guanine (G) heterocycle is most sensitive to oxidation, and this is reflected in a high incidence of mutations at this nucleotide in genomes experiencing oxidative stress.[5,7] Many products of G oxidation have been characterized, among which 8-oxo-7,8-dihydroguanine (OG) is a major product found in cells that causes G → T transversion mutations.[8,9] Beyond the mutagenesis of OG in a genome, there is a growing awareness that oxidation of G to OG in certain gene promoter sequences can modulate gene expression as a response to oxidative and inflammatory stress.[10−13] For instance, activation of proinflammatory genes,[14,15] *BCL2*,[16] *SIRT1*,[17] *VEGF*,[18,19] and *KRAS*,[20] by oxidation of G to OG in their promoter regions has been observed. These studies ascribe an epigenetic-like role to OG to regulate gene expression.[10−13] In the present report, we hypothesize and describe studies to support the proposal that the human *NEIL3* DNA repair gene can be activated by G oxidation to OG in a G-rich region of the promoter capable of folding into a G-quadruplex (G4).

Oxidative or inflammatory stress conditions in cell or animal model studies have identified an increase in *NEIL3* expression correlated with an increase in G oxidation to OG in the genome. For example, infection-induced colitis in mice was found to yield significantly higher levels of *NEIL3* in their livers in tandem with increased OG formed in the genome.[8] Hypoxia-ischemia in neural progenitor cells showed increased *NEIL3* expression and oxidative stress markers.[21] Myocardial infarctions result in elevated oxidative stress and DNA oxidation (i.e., OG),[22] as well as *NEIL3* induction.[23] Lung and colon cancers are associated with increased oxidative stress markers (e.g., OG)[24] and higher levels of *NEIL3* expression.[25] Lastly, hyperoxic reoxygenation in newborn mice increases *NEIL3* expression[26] and OG levels.[27] This wide variety of studies has found that oxidative stress or inflammation can lead to G oxidation to OG in the genome and induction of the *NEIL3* gene.

Received: February 17, 2019
Published: June 26, 2019

DOI: 10.1021/jacs.9b01847
J. Am. Chem. Soc. 2019, 141, 11036−11049

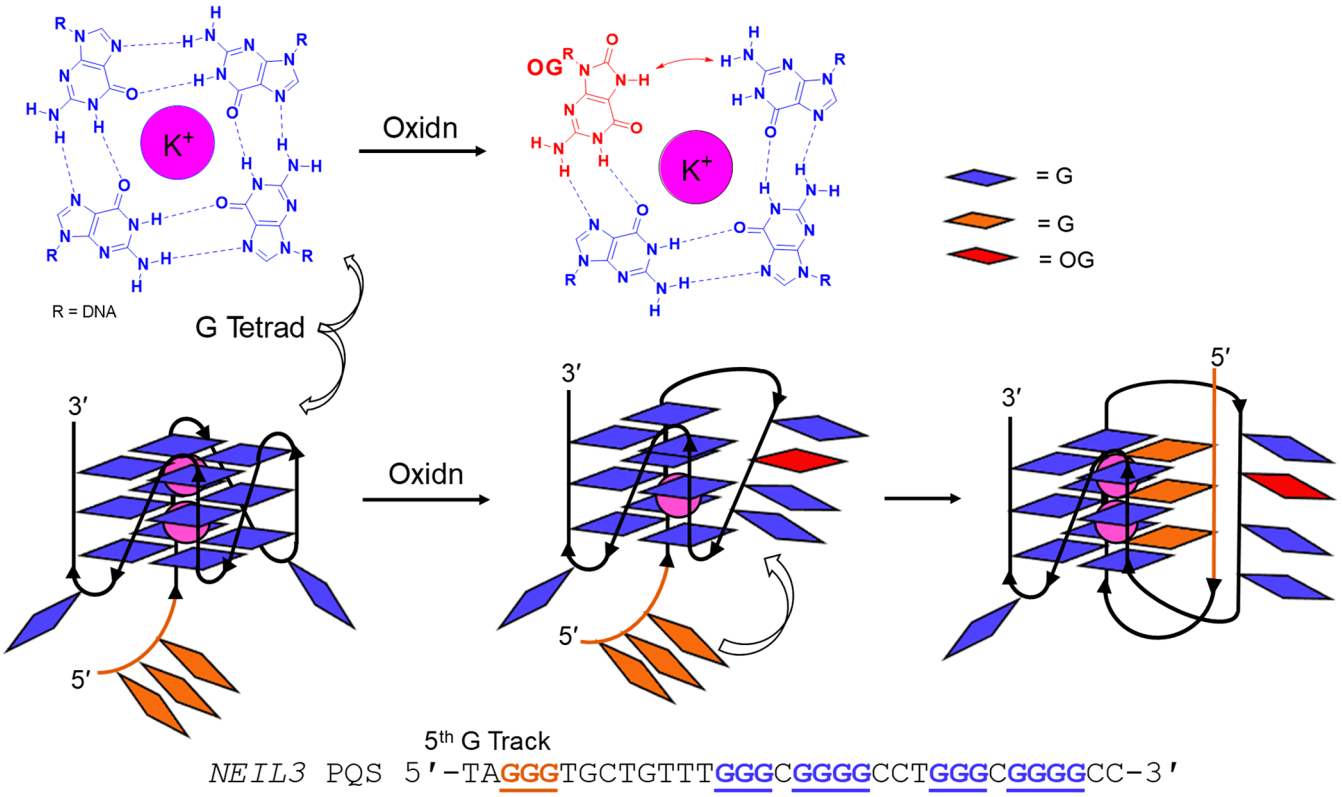

Figure 1. *NEIL3* PQS adopts a G4 fold that upon oxidative modification of a G tetrad engages the 5th G track to maintain a stable fold. (Top) Unfolding of a G tetrad upon oxidation of G to OG. (Middle) Cartoon depicting release of a damaged G track and swapping in of the 5th track to maintain a stable G4. (Bottom) Sequence of the *NEIL3* PQS from positions −34 to −3 in the coding strand, relative to the TSS.

We hypothesize that oxidation of G in the *NEIL3* promoter region may be responsible for guiding cellular pathways for activation of mRNA synthesis, and accordingly, a G-rich region of the promoter would be an excellent candidate site for oxidation to occur. Such a region exists;[28] the human *NEIL3* gene has a G-rich region in the coding strand of the promoter close to the transcription start site (TSS) that would be sensitive to oxidation. Additionally, as described later, this sequence is a potential G-quadruplex-forming sequence (PQS) that requires four G runs to adopt a G4 fold. G-Quadruplex folds are noncanonical DNA structures composed of G:G Hoogsteen base pairs that form stacked G tetrads from four closely spaced G runs.[29−31] The *NEIL3* PQS has an additional fifth G track.[28] Our previous studies found that this PQS adopts a G4 fold in which a chemical modification inhibiting Hoogsteen base pairing in a G tetrad is rescued by the fifth G track, swapping out the damaged strand to maintain the fold (Figure 1).[28,32] This flexibility in the sequence is essential for understanding the experiments conducted herein, in which a pathway is outlined that harnesses G oxidation to OG to initiate formation of a noncanonical G4 fold by engaging the base excision repair pathway (BER). The research described provides another example of a collaboration between DNA repair and gene activation.[33] This proposal is consistent with studies from our laboratory and others regarding a non-canonical DNA structure providing an avenue to gene activation via G oxidation to OG.[17,19,20,34] Finally, these results add additional support for the claim that the simple modification of G to OG yields a heterocycle to focus the BER process in DNA for regulation of transcription during oxidative or inflammatory stress.[10,11,13,15]

MATERIALS AND METHODS

DNA Strand Preparation. All DNA oligomers were synthesized and deprotected by the DNA/Peptide core facility at the University of Utah following standard protocols. The site-specific introduction of OG or the tetrahydrofuran analogue of an abasic site (F) was achieved using commercially available phosphoramidites. After synthesis and deprotection via standard protocols, the crude oligomers were purified using an anion-exchange high-performance liquid chromatography (HPLC) column running a mobile phase system consisting of A (1 M LiCl and 20 mM LiOAc at pH 7 in 1:9 MeCN/ddH_2O) and B (1:9 MeCN/ddH_2O). The method was initiated at 20% B and increased via a linear gradient to 100% B over 30 min with a flow rate of 1 mL/min while monitoring the absorbance at 260 nm. The purified samples were dialyzed against ddH_2O for 48 h, lyophilized to dryness, and resuspended in ddH_2O to make stock solutions. The concentrations of the samples were determined by measuring the absorbance at 260 nm, in which the nearest-neighbor approximation model was used to estimate the extinction coefficient. The extinction coefficients for the modified DNA strands were estimated by replacing G for OG and omitting a nucleotide for F. The oligomers were studied at the specified concentrations and buffers indicated for each experiment, as described for each experiment later.

DNA Preparation for Polyacrylamide Gel Electrophoresis Analysis. The purified DNA strands to be analyzed by polyacrylamide gel electrophoresis (PAGE) were radiolabeled with ^{32}P-ATP using T4 polynucleotide kinase following a literature protocol.[35] The radiolabeled samples were prepared differently for each experiment as outlined later.

Determination of Oxidation Sites and Products. All oxidations were conducted in 20 mM KP_i (pH 7.4), 120 mM KCl, 12 mM NaCl, with 10 μM DNA at 37 °C. Oxidation sites were determined on reactions doped with 20 000 cpm of 5′-^{32}P labeled strand in a 50-μL reaction utilizing the following oxidant conditions: Riboflavin (type I photooxidant) was added to give a 50 μM final

DOI: 10.1021/jacs.9b01847
J. Am. Chem. Soc. 2019, 141, 11036−11049

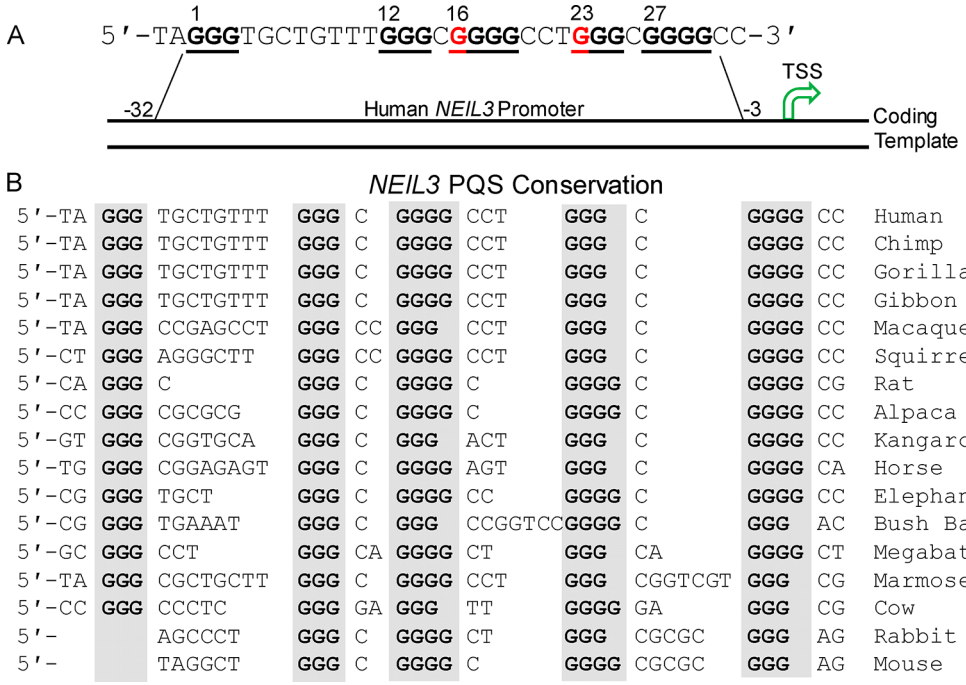

Figure 2. (A) Position and sequence of the *NEIL3* PQS. The G nucleotides shown in red at positions 16 and 23 were individually replaced with OG, as described later. (B) Alignment for this G-rich sequence in various mammals to demonstrate its conservation.

concentration followed by exposing the solution to 350 nm light for 0−15 min from a lamp (300 W) held 7 cm above the reaction tube with the lid left open. The $CO_3^{\bullet-}$ was produced when SIN-1 thermally decomposed to generate $ONOO^-$ (0, 3, or 5 mM) with 25 mM $KHCO_3$ present for 30 min. Following the oxidation, the samples were dialyzed against ddH_2O overnight and then lyophilized to dryness followed by addition of 200 μL of 1 M freshly prepared piperidine that was incubated at 90 °C for 2 h. The piperidine was removed by lyophilization. Next, the samples were resuspended in 12 μL of loading dye (30% glycerol, 0.25% bromophenol blue, and 0.25% xylene cyanol), and 6 μL was loaded on a 20% denaturing PAGE and electrophoresed at 75 W for 2.5 h. A Maxam−Gilbert G-lane was run alongside reaction lanes to determine the G oxidation sites. The cleavage sites were observed and quantified by storage-phosphor autoradiography on a phosphorimager.

The oxidation products were determined by nuclease and phosphatase digestion of the oxidized strands followed by reversed-phase HPLC (RP-HPLC) analysis of the liberated nucleosides. For analysis, reactions were conducted similarly to those described earlier with the exception of not adding the 5′-^{32}P labeled strand. For each oxidant studied, 20 reactions were conducted and then combined to have 10 nmol of oxidized DNA. Next, the samples were dialyzed overnight to remove the reaction buffer. After concentrating the samples by lyophilization, they were resuspended in 50 μL of digestion buffer and treated with nuclease P1, snake venom phosphodiesterase, and calf intestinal phosphatase, as previously described.[36] Finally, the products were quantified by RP-HPLC following a previously described protocol for which the entire process is detailed in the Supporting Information.[35]

Plasmid Construction. Modification of the plasmid to contain the *NEIL3* PQS in the promoter of a luciferase gene was achieved using a method previously outlined.[19] Synthesis of plasmids containing site-specifically incorporated OG or the AP model F was achieved following a previously established protocol.[19] Confirmation of the successful incorporation of the modification into the plasmids was performed by a gap ligation and Sanger sequencing protocol that we have reported.[37] The complete details of the synthesis and PCR primers used can be found in the Supporting Information.

Cell Studies. The human U87 glioblastoma cells were obtained from ATCC, and the mouse embryonic fibroblasts (MEFs) in the wild-type or $OGG1^{-/-}$ states were prepared as previously described.[38] All cells were grown in Dulbecco's modified Eagle medium supplemented with 10% fetal bovine serum, 20 μg/mL gentamicin, 1× glutamax, and 1× nonessential amino acids. The cells were grown at 37 °C with 5% CO_2 at ∼80% relative humidity and were split when they reached ∼75% confluence. The transfection experiments were conducted in white, 96-well plates by seeding 3×10^4 cells per well and then allowing them to grow for 24 h. After 24 h, the cells were transfected with 250−500 ng of plasmid per well using X-tremeGene HP DNA transfection agent (Roche) following the manufacturer's protocol in Opti-MEM media. The dual-glo luciferase assay (Promega) was conducted following the manufacturer's protocol 48 h post transfection on the basis of our previous work that found this analysis time provided maximal differentiation of the expression levels between the plasmids studied in these cell lines.[39] The APE1 siRNA knockdown experiments were conducted by treating U87 cells with 50 nM siRNA (Qiagen) 24 h prior to transfection of the plasmids. The transfection experiments were conducted at least four times, and the errors reported represent 95% confidence intervals.

The TNFα-induced oxidations of cells transfected with the *NEIL3* PQS-containing plasmids were conducted by first following the seeding procedure described earlier. After allowing the U87 cells to grow for 24 h, they were treated with TNFα at a concentration of 20 ng/mL for 0, 30, 60, or 120 min. Upon completion of the TNFα incubation, the cells were washed with phosphate-buffered saline (PBS) twice to remove the cytokine, and then Opti-MEM media was placed in the wells to allow the cells to grow for 48 h prior to conducting the dual-glo luciferase assay as described earlier.

APE1 Activity Assays. The APE1 assays were conducted by addition of APE1 (1 U/reaction; NEB) to a 10 nM solution of substrate DNA in a 10-μL reaction composed of 1× APE1 buffer (NEB; 50 mM KOAc, 20 mM Tris pH 7.9, 10 mM $Mg(OAc)_2$, and 1 mM dithiothreitol (DTT)). The reactions were allowed to proceed for 1, 5, 10, 30, or 60 min at 37 °C before termination. The reactions were terminated by a 10-μL bolus addition of stop buffer (95% formamide, 10 mM NaOH, 10 mM EDTA, 0.1% xylene cyanol, and 0.1% bromophenol blue) followed by heating the mixture at 65 °C for 20 min. Assay mixtures without enzyme were used as negative controls. After denaturing the samples at 95 °C for 10 min, the samples were then analyzed via separation on a 20% denaturing PAGE

DOI: 10.1021/jacs.9b01847
J. Am. Chem. Soc. 2019, 141, 11036−11049

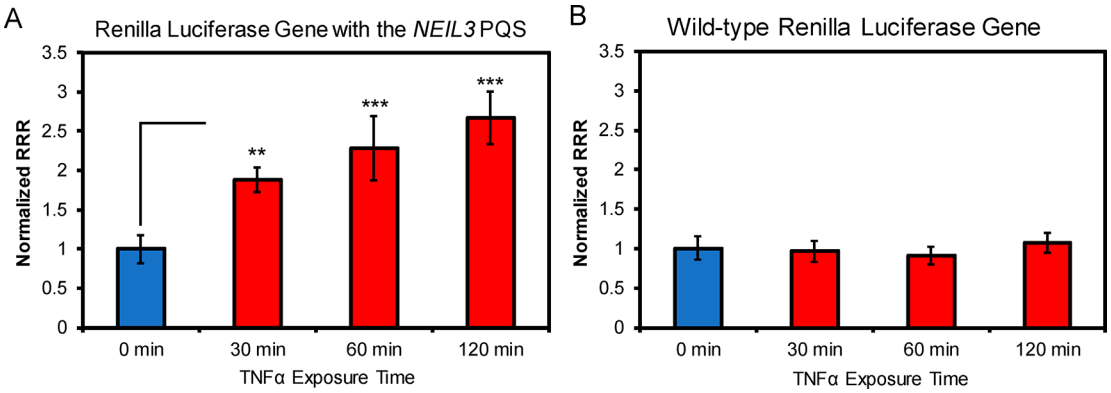

Figure 3. Luciferase expression from a reporter plasmid transfected into U87 cells treated with TNFα at various times. (A) Reporter plasmid containing the five-track *NEIL3* PQS in the coding strand of the promoter for the Renilla luciferase gene at position −16 relative to the TSS and (B) the reporter plasmid in the wild-type state without the PQS. The plasmid contains two luciferase genes, in which the firefly gene remained in the wild-type state in both studies to be used as an internal standard for data analysis. The relative response ratio (RRR) = (Renilla expression)/(firefly expression) measured by a dual-glo luciferase assay is reported in the graphs. The values are normalized to the same plasmid without exposure to TNFα. Levels of significance were determined by a Student's *t* test in which $^{**}P < 0.01$ and $^{***}P < 0.001$.

run at 45 W for 2 h. After electrophoresis, the gels were placed in a phosphorimager screen for 18 h, and the bands were visualized using storage-phosphor autoradiography. The band intensities were quantified using ImageQuant software. Each reaction was conducted in triplicate to obtain the reported errors that represent the standard deviation of the measurements.

Circular Dichroism Analysis. The prefolded G4 samples were annealed at a 10 μM concentration in 20 mM lithium cacodylate buffer (pH 7.4) with 140 mM KCl and 12 mM NaCl. The samples were placed in a 0.2 cm quartz cuvette for circular dichroism (CD) analysis at 20 °C. The recorded data were solvent background subtracted and then normalized on the *y*-axis to units of molar ellipticity ([Θ]) for plotting and comparative purposes.

Thermal Melting Analysis. The thermal melting (T_m) values were determined on samples of 5 μM oligomer in buffered solutions with physiological K^+ and Na^+ concentrations (20 mM lithium cacodylate pH 7.4, 140 mM KCl, and 12 mM NaCl). The melting experiments were initiated by thermally equilibrating the samples at 20 °C for 10 min followed by heating at 0.5 °C/min and equilibrating at each 1 °C increment for 1 min. Readings at 260 and 295 nm were taken after each 1 °C change in the temperature from 20 to 100 °C. Plots of absorbance at 295 nm versus temperature were constructed, and the T_m values were determined by a two-point analysis protocol using the instrument's software.

Bioinformatic Analysis. The Flag-tagged OGG1 ChIP-Seq results were obtained from the NCBI's Gene Expression Omnibus via accession number GSE89017.[40] All analyses were conducted on the web-based instance of Galaxy.[41] The sequencing reads were aligned to hg[38] using Bowtie2 with the default parameters,[42] and the peaks of 4-fold or more enrichment were called using MACS2 with the broad peaks option selected and all other parameters left as the default.[43] The peak locations identified were converted to fasta files for analysis of PQSs using a modified version of QuadParser in which the loop lengths were allowed to extend up to 12 nucleotides.[44] The genomic locations for all peaks were determined using the PAVIS tool.[45]

RESULTS AND DISCUSSION

Reporter Gene Bearing the Promoter *NEIL3* PQS Induced by In Cellulo Stress. The human *NEIL3* gene possesses a PQS in the coding strand of the promoter starting at position −3 from the TSS (Figure 2A).[28] Formation of a G4 fold requires four G-runs, and this particular PQS possesses five G-runs, as we previously reported.[28] The previous results identified the four G-tracks on the 3′ side to be the principle G4 fold; additionally, the fifth G-run was engaged in yielding a more stable fold when one of the principle G nucleotides was oxidatively modified.[28,32] The interesting new observation regarding this sequence is the conservation of the PQS in a wide selection of mammalian genomes that have been sequenced and deposited in the Ensemble Genome Browser (Figure 2B). Humans, chimps, gorillas, and gibbons retain the *NEIL3* PQS without any nucleotide changes, while modifications predominantly at nucleotides between the G runs (i.e., loop regions) were observed in the other genomes inspected. The conservation of the *NEIL3* PQS and the retention of the ability for this region to be capable of G4 folding in this group of mammals support the proposal that this sequence was favorably selected.

We hypothesize that the *NEIL3* PQS is prone to oxidation in a cellular genome under conditions of oxidative or inflammatory stress, directing G oxidation to the promoter and guiding BER-dependent gene activation. To first address this hypothesis, the *NEIL3* PQS was synthesized into the coding strand of a promoter regulating a luciferase gene in a reporter plasmid. This enabled transfection of the plasmid into human glioblastoma cells (U87) and induction of stress while monitoring the luciferase expression. This experiment provided an understanding of whether the presence of the *NEIL3* PQS in a gene promoter could function to activate transcription during stress as previously identified in a variety of cell or animal models.[8,21−23,25,26] The reporter plasmid selected has two luciferase genes wherein the Renilla luciferase gene carried the modified promoter with the *NEIL3* PQS, and the firefly luciferase gene was not altered and used as an internal standard for better quantification of expression changes via a dual-glo luciferase assay. The cells were stressed with TNFα (20 ng/mL) for 0, 30, 60, and 120 min following a previously reported protocol.[15] The TNFα cytokine induces an inflammatory response, in which $O_2^{\bullet-}$ and NO production are upregulated, allowing them to react to yield $ONOO^-$.[46] In the cellular context, $ONOO^-$ further reacts via a multistep pathway with CO_2 and ultimately decomposes to $CO_3^{\bullet-}$ and $^{\bullet}NO_2$.[1] Carbonate radical selectively oxidizes the G heterocycle and does not damage the sugar−phosphate backbone of DNA.[47] When the Renilla luciferase expression was monitored and normalized to the internal control (i.e., firefly luciferase) during the time-course exposure to TNFα, the amount of

DOI: 10.1021/jacs.9b01847
J. Am. Chem. Soc. 2019, 141, 11036−11049

Scheme 1. Proposed Mechanism for Activation of Transcription upon Oxidative Modification of a G Nucleotide to OG in the Context of a Promoter PQS in the Coding Strand near the TSS[a]

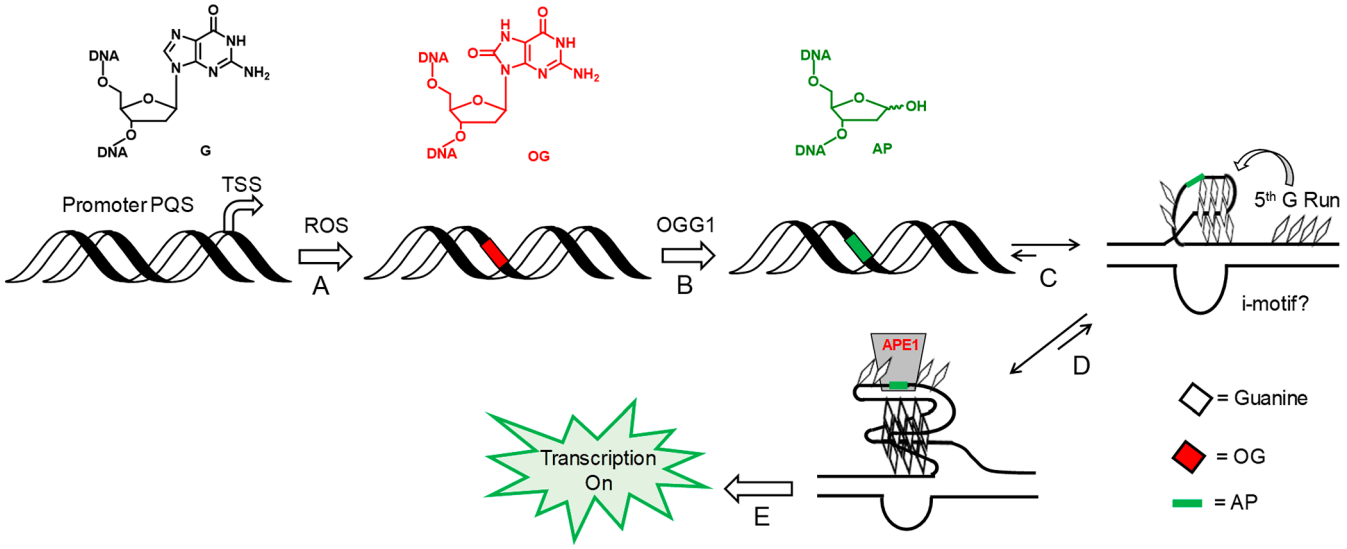

[a]The proposal was previously suggested and supported for the *VEGF* PQS.[19] In the present work, we hypothesize that a similar pathway is invoked for induction of the *NEIL3* gene under oxidative stress or inflammation conditions. The capital letters below the reaction arrows will be used to guide a discussion regarding the additional experiments conducted.

Scheme 2. Outline of G Oxidation Products and the Extent To Which They Are Oxidized Relative to G[a]

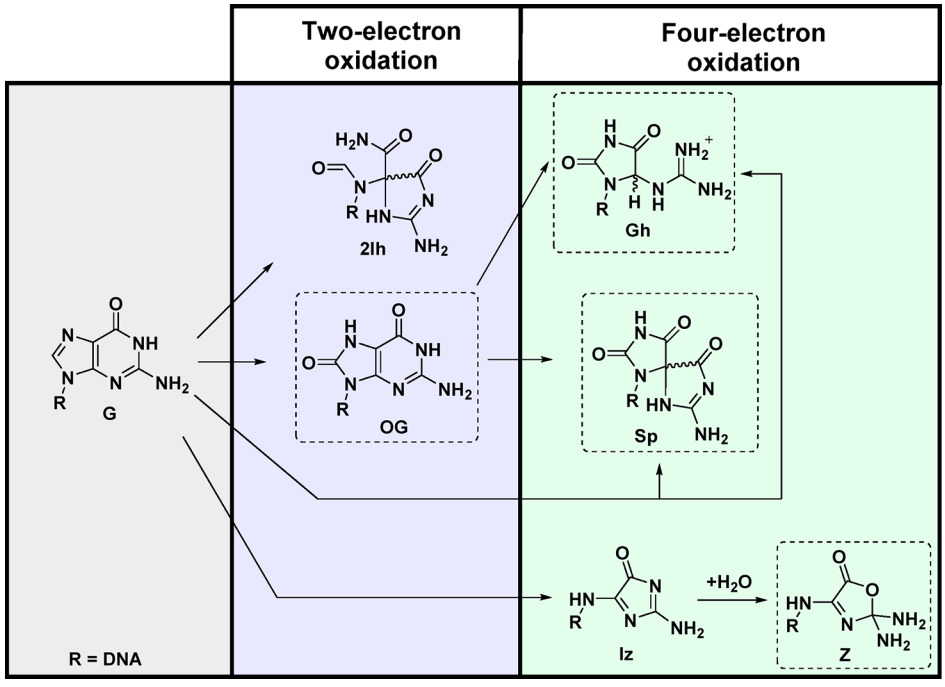

[a]The products in dashed boxes were detected in the present studies.

Renilla expression increased significantly with a dependency on the exposure time (Figure 3A red). After 120 min of TNFα exposure, the increase in Renilla expression reached nearly 3-fold. Two controls were conducted; in the first, the *NEIL3* PQS-containing plasmid was transfected into U87 cells that were not treated with TNFα, and no significant increase in expression was observed (Figure 3A blue). In the second control experiment, U87 cells were transfected with the dual-luciferase plasmid that was not modified with the *NEIL3* PQS and then exposed to TNFα. In this experiment, no significant increase in Renilla luciferase expression was observed (Figure 3B). Taken together, these intriguing observations suggest that the *NEIL3* PQS may have been oxidized at a G nucleotide, leading to Renilla luciferase induction. This observation is consistent with the previous cell and animal model studies that found *NEIL3* expression increased under oxidative stress conditions.[8,21−23,25,26]

Proposed Mechanism for *NEIL3* Activation Under Oxidative Stress Conditions. Previous work in our laboratory focused on activation of transcription for the

DOI: 10.1021/jacs.9b01847
J. Am. Chem. Soc. 2019, 141, 11036−11049

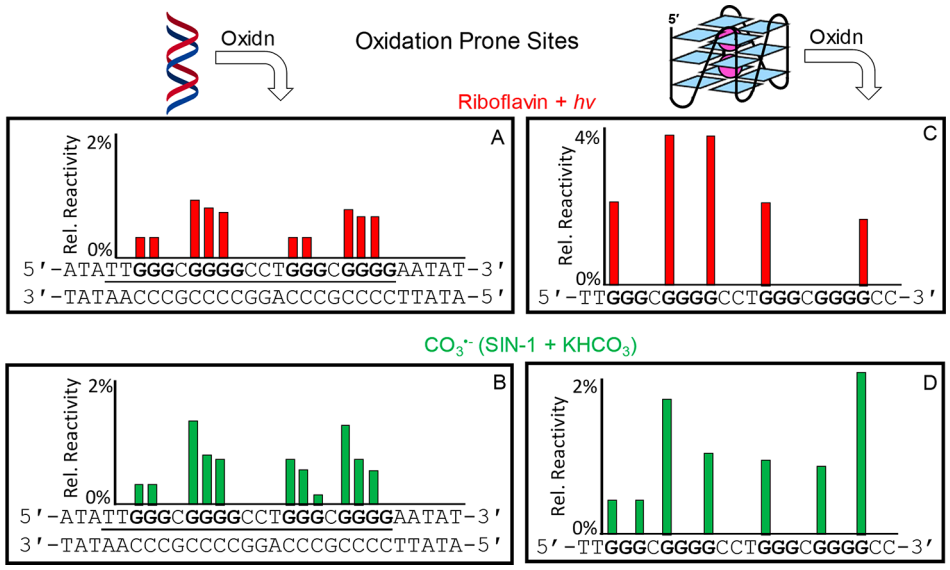

Figure 4. Sites of riboflavin-mediated (A, C) or $CO_3^{\bullet-}$-mediated (B, D) oxidation in the *NEIL3* four-track PQS folded as a duplex with the complementary strand or a G4. The oxidized sites were identified by hot piperidine cleavage and denaturing PAGE analysis post-oxidation. The reactions were conducted under low conversion conditions (<10%) to achieve single-hit chemistry. The bars represent the average of triplicate measurements with associated errors of ~10% of the values reported. See Figure S1 for the data and details regarding the analysis.

VEGF gene under oxidative stress conditions that bears a native PQS in the coding strand within 50 bps of the TSS.[19,39] These previous studies took a chemical approach to demonstrate oxidative modification of a G nucleotide to OG in the *VEGF* PQS context activated transcription (Scheme 1). In the first step of the proposed mechanism, the *VEGF* PQS in the dsDNA conformation is oxidatively modified at a G nucleotide to yield OG. Next, removal of OG by OGG1 yields an AP that destabilizes the dsDNA, providing the thermodynamic drive to shift the equilibrium to a G4 fold, placing the AP in a loop of the G4. A loop placement of the AP in this sequence was enabled by the presence of a fifth G run that could swap with the AP-containing G run and facilitate strong G4 folding.[48] Additionally, this presents the AP to APE1 in a loop context that is bound by the protein while the catalytic ability to cleave the strand is attenuated.[49] Previous studies support the idea that, when APE1 is stalled on DNA in a promoter, recruitment of activating factors occurs, leading to increased gene expression when the modifications are in the coding strand close to the TSS (Scheme 1).[17,19] The Gillespie laboratory took a biological approach to studying *VEGF* activation under hypoxic conditions in pulmonary cells involving G oxidation and BER activation,[18] and our proposal is consistent with their findings. In the present work, activation of the *NEIL3* gene via a similar mechanism was probed and supported in the studies described next.

First, experiments were designed to understand the oxidation chemistry that occurs in the *NEIL3* PQS under cellular stress conditions (Scheme 1A). A set of in vitro oxidations of synthetic *NEIL3* PQSs were conducted to identify sites sensitive to oxidation and the products formed. Two model oxidants were selected for interrogation. The first oxidant was the type I photooxidant riboflavin, which is a G-selective, one-electron oxidant harnessed to mimic oxidative stress conditions. During the photoredox catalytic cycle of riboflavin under aerobic conditions, $O_2^{\bullet-}$ is produced that can react with oxidized G intermediates. The mechanistic details of the oxidation have been reported.[4,50] The second oxidant selected for study was the $ONOO^-$ generator SIN-1 that thermally decomposes in the presence of $KHCO_3$ to ultimately yield the G-specific oxidant $CO_3^{\bullet-}$.[1] A hallmark of inflammatory stress is overproduction of $ONOO^-$ that can decompose in the cellular matrix to yield $CO_3^{\bullet-}$.[1] These two oxidants have been previously reported to yield the G oxidation products OG, spiroiminodihydantoin (Sp), 5-guanidinohydantoin (Gh), and 2-iminohydantoin (2Ih), as well as 2,5-diaminoimidazolone (Iz) and its hydrolysis product 2,2,4-triamino-2*H*-oxazol-5-one (Z; Scheme 2).[4,50,51] Formation of Sp and Gh can also occur via a second oxidation of OG that readily occurs because of the low reduction potential of OG.[52,53] The products OG, Sp, Gh, and Z have been identified in animal models or prokaryotes.[8,54,55] Furthermore, the heterocyles Sp, Gh, and 2Ih are excellent substrates for the NEIL BER glycosylases.[4]

Oxidations were conducted with the *NEIL3* PQS folded as dsDNA with the C-rich complementary strand present or as a G4 when the C-rich strand was absent. The sequences studied in the dsDNA versus the G4 contexts differed slightly; additionally, both studies interrogated the four G-track *NEIL3* PQS. In the G4 context, two nucleotides of the natural 5′ and 3′ tails were maintained to provide a more natural sequence context; the importance of tail nucleotides impacting the topology of a promoter G4 was previously demonstrated in our laboratory.[56] In the dsDNA context, five A:T base pairs were placed on the 5′ and 3′ sides of the PQS to enhance the duplex stability and facilitate the study of G oxidation in a well-formed duplex while avoiding any unanticipated effects associated with end fraying. The reaction conditions modeled the ionic strength and monovalent cation composition of a human cell (140 mM K^+ and 12 mM Na^+) that are favorable for G4 folding because of the high level of K^+ ion present.[29] The oxidations were conducted under single-hit conditions (<10% yield) to reveal the G nucleotides most prone to react. The sites were found via hot piperidine cleavage visualized by sequencing PAGE analysis using conditions previously established to cleave the common G oxidation products

DOI: 10.1021/jacs.9b01847
J. Am. Chem. Soc. 2019, 141, 11036−11049

observed with the oxidants selected for study, with the exception of OG.[57] Identification of the location of OG was achieved by treating the oxidized strands with Na_2IrCl_6 to drive the oxidation of OG to the piperidine-labile products Sp or Gh (Scheme 2) following our previously reported protocol.[58]

The PAGE analysis revealed that when the *NEIL3* PQS was folded as dsDNA, G nucleotides 5′ to another G nucleotide were most sensitive to oxidation with the photooxidant riboflavin or $CO_3^{\bullet-}$ (parts A and B of Figure 4 and Figure S1). In the three or four G nucleotide runs, the 5′-most G provided the greatest reactivity, and those 5′ to another G were reactive with slightly less intensity. The 5′ G effect for sensitivity to oxidation has been widely documented,[59−61] and the present results are consistent with the previous observations. In contrast, when the *NEIL3* PQS was folded as a G4, the G nucleotides sensitive to oxidation were on the 5′ end of G runs in the core of the G4 fold or G's found in the loop regions between the core G nucleotides (Figure 4C and D). The present observations are consistent with prior studies with other sequences.[35,48] The core versus loop designations are based on the sequence—when only three G's are in a run, they are all needed for G4 folding; therefore, they are core G nucleotides. Those runs with four G's can shift when oxidized to place either the 5′- or 3′-most G in a loop position. This shifting of a G run occurs because oxidatively modified G nucleotides cannot participate in Hoogsteen G:G base pairing in the core (Figure 1); thus, a terminal G in a four-G run will be in a loop position. The G nucleotides sensitive to oxidation were similar for both oxidants studied, with the $CO_3^{\bullet-}$ hitting slightly more G nucleotides than the photooxidant (Figure 4C and D). Also noteworthy is the observation that middle G's in a run of 3 or 4 G's are not very reactive in the G4 fold although they are in a B helix. This is likely due to the lower stability of a G radical cation in close proximity to two K^+ cations; hence, the electron hole migrates in the base stack to the 5′ G.[35]

Another study conducted was to perform the oxidations under reducing conditions that mimic the cellular context. Prior to the oxidations, 3 mM *N*-acetylcysteine (NAC) was added to the reaction to model cellular glutathione. NAC was selected because it has a free thiol similar to glutathione while the nucleophilic primary amine is blocked by the acetyl group to prevent NAC from forming adducts with oxidized G nucleotides.[62] Oxidations with NAC present did not impact the sites of riboflavin-mediated oxidation, while the $CO_3^{\bullet-}$ oxidations were completely quenched under the reducing conditions studied (Figure S2). In their entirety, these experiments probed the sensitivity of the *NEIL3* PQS toward oxidation and provide details regarding the first step in the activation process illustrated in Scheme 1A.

To better understand the chemistry of the oxidation, the products were determined and quantified via nuclease and phosphatase digestion of the oxidized strands followed by RP-HPLC analysis utilizing a protocol we previously reported (Figure S3).[35,36] Riboflavin-mediated oxidations of the *NEIL3* PQS without NAC present furnished Gh (∼40%) as the major product in dsDNA contexts, while in the G4 context, Sp (∼40%) and Z (∼50%) were the major products detected (Figure 5). Under nonreducing conditions, $CO_3^{\bullet-}$ oxidation of the *NEIL3* PQS found that Gh (∼60%) was the major product in dsDNA contexts and Sp (∼70%) was the major product in the G4 context (Figure 5). These findings are consistent with previous reports.[35,48] Next, when the riboflavin-mediated

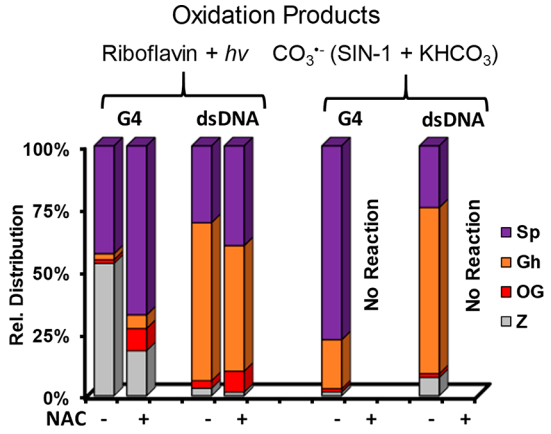

Figure 5. Relative product distributions observed from oxidation of the *NEIL3* PQS folded as a G4 or a duplex with the complementary strand. Oxidation product distributions were determined by nuclease and phosphatase digestion of the oxidized strands followed by RP-HPLC analysis for identification and quantification following a previously reported protocol.[35,36] The values represent averages for triplicate analyses, and the errors represent ∼10% of the reported values. See Figure S3 for details regarding the analysis.

oxidations were conducted in the presence of 3 mM NAC, the amount of Z decreased the most, by 4.6-fold, while the levels of OG increased the most, by 6.3-fold, followed by the OG hyperoxidation product Sp that increased 1.5-fold when compared to reactions devoid of NAC. This observation is consistent with a previous study[35] which found that NAC quenches the $O_2^{\bullet-}$ intermediate involved in the proposed mechanism for formation of Iz/Z.[63] The hyperoxidation of OG to Sp or Gh readily occurs as a result of the low reduction potential of OG relative to G (OG = 0.74 V and G = 1.29 V, both values vs NHE at pH 7);[64] thus, when OG is present in an oxidation reaction, this heterocycle will be further oxidized when the yields are pushed higher for product analysis, leading to an underestimate of the amount of OG formed.[52,53] We expect that cellular OG levels will be nearly 2 orders of magnitude greater in concentration than Sp or Gh that was previously demonstrated in the colon or liver of mice with infection-induced colitus.[8] The analytical method is capable of detecting Fapy-dG and 2Ih;[65] however, neither product was observed in the present reactions. The present observations suggest that OG is the favored oxidation product under reducing reaction conditions, similar to the cellular context.[8] Lastly, NAC quenched the $CO_3^{\bullet-}$ oxidations; hence, products were not observed. These studies identify products formed from oxidation of the *NEIL3* PQS, providing insight into the chemistry proposed in Scheme 1A.

The previous in vitro studies identified the likely sites at which the *NEIL3* PQS would be prone to oxidation and the products formed in genomic DNA of cells under oxidative stress conditions (Figures 4 and 5). This knowledge enabled synthesis of a G oxidation product at sensitive sites in the *NEIL3* PQS-containing luciferase reporter plasmid to be transfected into U87 cells to determine whether oxidation of G in this promoter context impacts expression. The OG was incorporated at either of two reactive positions on the basis of the observations in Figures 4 and 5, one at position 16, which would occupy a loop position in the folded *NEIL3* G4, and the other at position 23, which would occupy a core position in the folded *NEIL3* G4 (Figure 2A). The presence of the fifth G

DOI: 10.1021/jacs.9b01847
J. Am. Chem. Soc. 2019, 141, 11036−11049

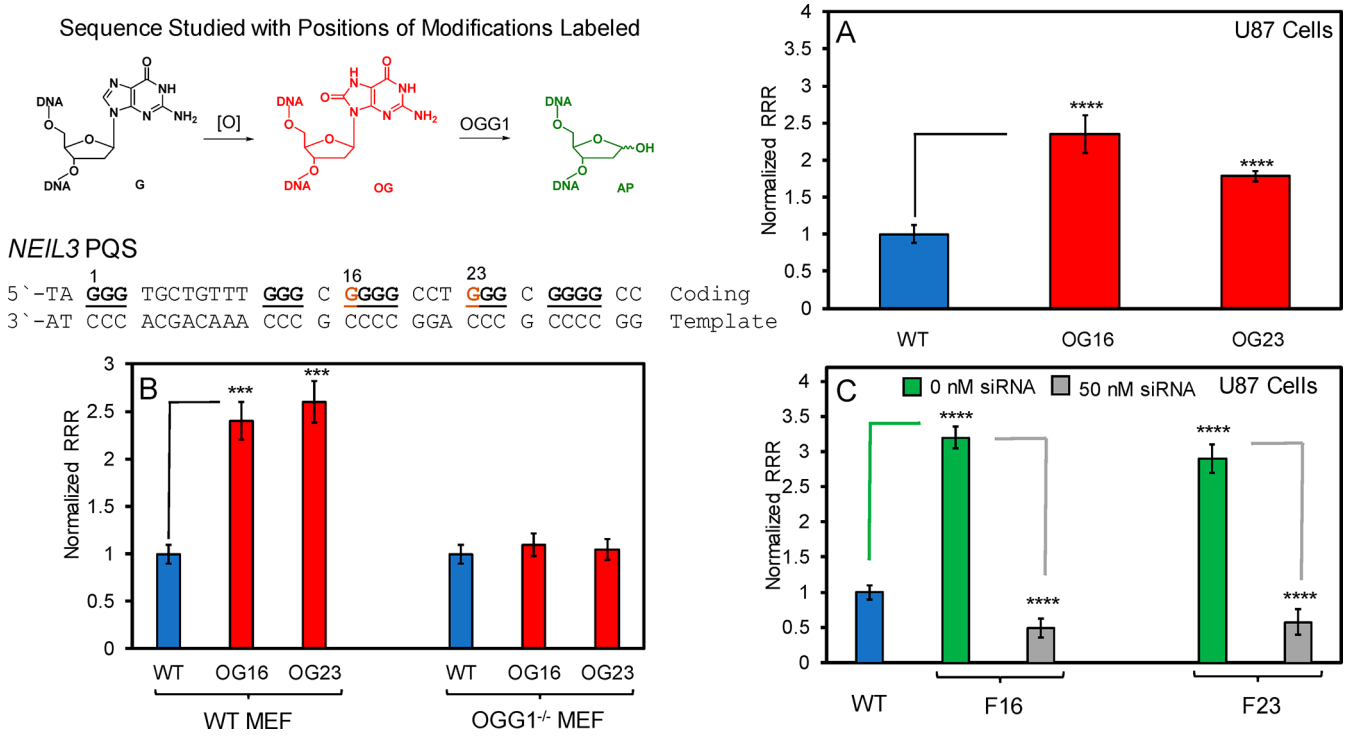

Figure 6. Impact on expression in mammalian cells when OG or an AP analogue (F) is synthetically installed in the *NEIL3* PQS in a reporter plasmid. Synthetic plasmids with OG synthetically installed in the *NEIL3* PQS context studied in (A) U87 cells or (B) mouse embryonic fibroblasts (MEFs) in the wild-type or OGG1$^{-/-}$ states. (C) Studies with plasmid that were synthesized with F in the *NEIL3* PQS context in U87 cells with and without siRNA to knockdown APE1 expression. A dual-glo luciferase assay to measure Renilla luciferase expression from the modified promoter and firefly luciferase from the unmodified promoter (i.e., internal standard) was conducted to report normalized RRRs. The values reported represent the average of quadruplicate trials, and the error bars represent 95% confidence intervals calculated using the Student's *t* test in which ***$P < 0.001$ and ****$P < 0.0001$. The measurements were taken 48 h post transfection.

track allows extrusion of a modification into a large loop (Figure 1).[32] Upon transfection and incubation of these site-specifically modified plasmids in U87 cells, the impact of oxidation on mRNA synthesis could be quantified via the luciferase reporter expression. Comparison of the oxidatively modified plasmids to the wild-type plasmid found that the presence of OG at a loop position resulted in a 2-fold increase in Renilla expression and that of OG at a core position furnished a 2.5-fold increase in Renilla expression (Figure 6A). The direction and magnitude of increased luciferase expression for these chemically defined experiments are similar to the findings when the *NEIL3* PQS-containing plasmid with only G nucleotides was transfected into U87 cells stressed with TNFα (Figure 3A), providing strong evidence that the promoter G4 sequence is oxidized after exposure to TNFα. These findings are also consistent with the cell and animal model studies which showed that *NEIL3* expression increases under oxidative stress or inflammatory conditions.[8,21−23,25,26] Lastly, this chemically defined plasmid allowed the demonstration that OG in the *NEIL3* PQS context in a gene promoter can induce mRNA synthesis in a human cell line.

The studies to this point established that oxidation of the *NEIL3* PQS in a promoter, whether induced by oxidative stress or synthetically installed, can activate mRNA synthesis. The next experiments provide details regarding the primary protein readers and structure-switching capability of the PQS to a G4, leading to upregulation of transcription. First, OG is expected to be removed from the *NEIL3* PQS in the dsDNA context by OGG1 to furnish an AP (Scheme 1B). A previous cell-based experiment demonstrated that OGG1 is generally a monofunctional glycosylase in vivo that yields an AP upon OG removal.[66] Exploration of the importance of OGG1 in this reaction was determined via transfection of the OG-containing *NEIL3* plasmids into wild-type and OGG1$^{-/-}$ MEFs. When the MEFs were in the wild-type state, the presence of OG in the *NEIL3* PQS in the transfected plasmids led to a similar increase in expression as observed in the U87 cells (Figure 6B). In contrast, transfection of the same OG-containing plasmids in the OGG1$^{-/-}$ MEFs yielded similar expression as observed for the non-OG containing plasmid (Figure 6B). This observation supports the critical role for OGG1 in the gene activation process after the *NEIL3* PQS is oxidatively modified at a G to yield OG (Scheme 1B).

Studies to probe the role of AP in the activation process were then conducted (starting at Scheme 1C). To understand the importance of AP formed from OG release from the *NEIL3* PQS, plasmids were synthesized with the AP analogue F (i.e., THF) that is processed by enzymes similarly to an AP with the benefit of being hydrolytically stable, unlike a native AP.[67] These strands were transfected into U87 cells and were found to yield increased Renilla luciferase expression relative to the wild-type *NEIL3* PQS-containing plasmid (Figure 6C). This observation supports the claim that an AP site is important for gene activation when the PQS was oxidatively modified, and the AP likely functions in the gene-activation process (Scheme 1C).

The next step of the mechanism involves an AP-mediated structural transition from dsDNA to a G4 fold (Scheme 1C). Support for this step in the proposal is derived from a series of thermal melting studies (T_m) on synthetic DNA strands with

DOI: 10.1021/jacs.9b01847
J. Am. Chem. Soc. 2019, 141, 11036−11049

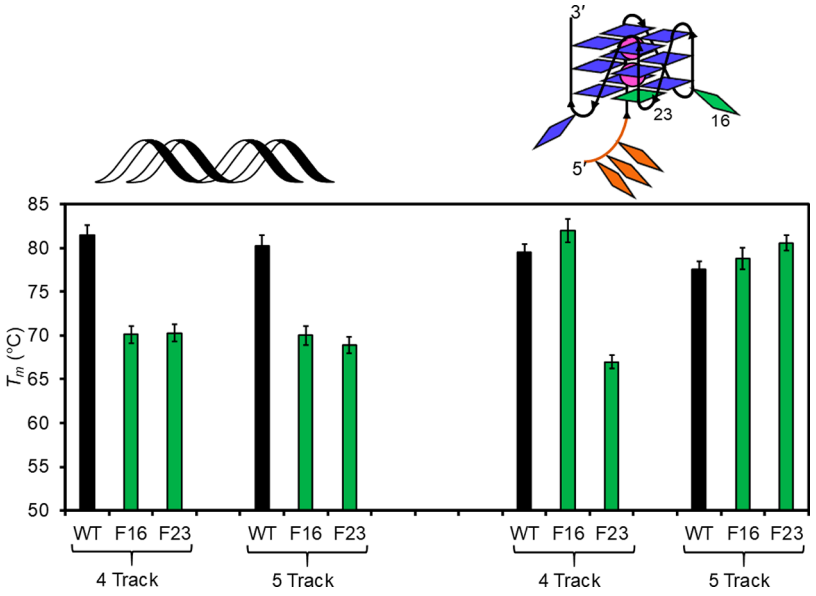

Figure 7. Plots of the T_m values for the four- and five-track *NEIL3* PQSs with an AP analogue F present in the dsDNA or G4 contexts. The values were determined from the thermal denaturing curves monitored at 295 nm, and the plots represent the average of triplicate measurements with the error bars representing standard deviations from these measurements.

the F analogue of an AP installed at each of the two positions chosen for study. Additionally, the *NEIL3* PQS was studied with four or five G tracks for comparison. The T_m value for the native four G-track *NEIL3* PQS as a duplex was 81.5 °C, and a similar value for the G4 was measured (79.5 °C; Figure 7). When the AP analogue F was studied in dsDNA, the T_m values decreased by ∼10 °C regardless of the position in which the F was studied. This observation is consistent with a previous study in G-rich sequences similar to the *NEIL3* PQS.[19] The presence of the F at a core position in the four G-track *NEIL3* G4 gave a T_m value of 67.1 °C, which is 13 °C lower than the native G4 fold. On the other hand, having an F at a loop position provided a T_m value 3 °C higher than the native G4. This observation suggests that prohibiting a G in a run of four G nucleotides from participating in the core of a G4 fold decreases the number of possible structures and slightly stabilizes the fold. When the five-track *NEIL3* PQS was studied in the dsDNA context, the F-bearing strands had a ∼10 °C lower T_m value than the native sequence. The interesting observation was with respect to the G4 context, in which regardless of the position of F, the T_m values were maintained similarly to the native G4 fold. Further, these T_m values were greater than (∼10 °C) the dsDNA context of the same sequence with the F modification. The ability of the fifth G-track to maintain the stability of the G4 when a modification was present is consistent with previous findings from our laboratory.[32] In summary, this observation supports a scenario in which the G4 fold is more stable than the duplex fold when an AP is present, and it suggests that the sequence can undergo a structural transition (i.e., B → G4) when the AP is present (Scheme 1C).

Support for a G4 fold in the gene-activation process is derived from previous studies.[19,39] In the work we conducted with the *VEGF* PQS located at the same position in this plasmid relative to the TSS, when the sequence was judiciously mutated to be incapable of adopting a G4 fold, gene activation was abolished when OG or an AP (i.e., F) was present.[19] A similar observation was reported in a follow-up study in more cell lines.[39] Additionally, the *NEIL3* PQS in the native state in this same plasmid and cell line was found to be activated by the G4-specific ligand Phen-DC3;[28] additionally, the *NEIL3* gene containing only one PQS[28] was activated in mammalian cell models treated with an anthraquinone derivative specific to G4s;[68] both studies support the proposal that the *NEIL3* PQS adopts a G4 with a ligand in cells. These results may be complicated by the ability of G4 ligands to also bind the i-motif fold in the C-rich complementary strand.[69] Lastly, *NEIL3* expression is upregulated during the S phase of the cell cycle,[70] which is when G4 folds predominantly occur.[71] The reports described are consistent with G4 folding occurring during the gene-activation process (Scheme 1C), which is further supported by the next set of experiments conducted.

In the final step of the proposed mechanism, the AP in the G4 context is bound by APE1 and poorly cleaved, resulting in gene activation via the trans-acting function of this protein (Scheme 1D). Previously, our laboratory and others have conducted cell-based studies to demonstrate the importance of APE1 in the activation process by stalling on AP in a non-B-form DNA structure such as G4 or hairpin.[17,19,39] Confirmation of the importance of APE1 in the current study was verified by treating the cells with 50 nM siRNA targeting the APE1 mRNA to knockdown the protein expression levels prior to plasmid transfection following a reported method.[19,39] The siRNA-treated cells produced highly attenuated expression of the Rluc gene compared to nontreated cells that supports the importance of APE1 in mediating gene expression (Figure 6C).

In a set of in vitro experiments, a final set of studies demonstrates that APE1 poorly cleaves an AP in a non-canonical structure such as the *NEIL3* PQS folded as a G4, while efficiently cleaving an AP in the same sequence folded as dsDNA. The in vitro enzymatic study compared the structural fold context and the role of the four- versus five-track G4 in altering the activity of APE1 (Scheme 1E). The reaction conditions for APE1 were recommended by the supplier (NEB) to include 50 mM KOAc in Tris buffer at pH 7.9;

DOI: 10.1021/jacs.9b01847
J. Am. Chem. Soc. 2019, 141, 11036−11049

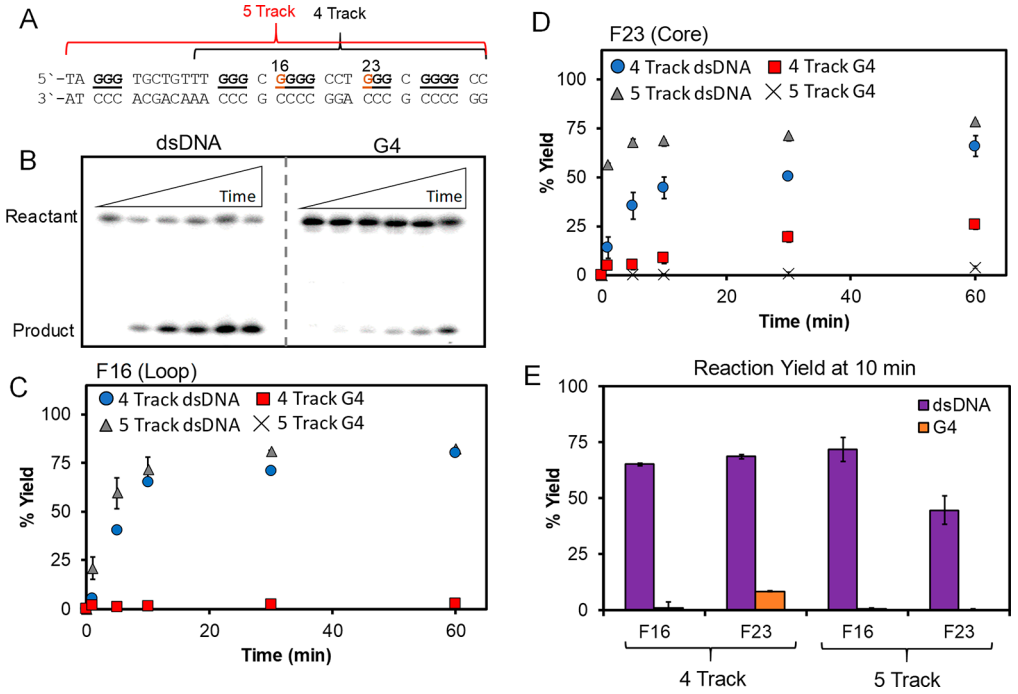

Figure 8. APE1-mediated cleavage of an AP analogue F at two different positions in the *NEIL3* PQS context folded as dsDNA or a G4. (A) Sequences studied with the positions of F identified. (B) Contrast-enhanced PAGE analysis of APE1-mediated cleavage of F at a core position in the four-track *NEIL3* PQS in the dsDNA or G4 folds showing the time evolution of product formation from 0−60 min. The complete and unenhanced PAGE along with all the data are present in Figure S5. (C, D) Profiles for the product evolution of APE1 cleavage of *NEIL3* PQSs with F at two different locations in either the dsDNA or G4 contexts. (E) Plot of reaction efficiency for each study at 10 min for comparative purposes. Note that the symbols X in (C) lie directly behind the red squares.

therefore, the *NEIL3* G4s were first demonstrated to fold under these reaction conditions by circular dichroism (CD) spectroscopy and T_m analysis. These confirmatory experiments found nearly identical CD spectra between the suggested APE1 reaction conditions and conditions modeling the cellular context (140 mM K^+, 12 mM Na^+, pH 7.4; Figure S4). The major difference observed was lower T_m values (~10 °C) for the *NEIL3* G4 folds in the APE1 buffer resulting from the lower ionic strength (Figure S4). Nonetheless, the T_m values (>55 °C) were significantly above the APE1 reaction temperature of 37 °C, suggesting that the G4s are folded during the reactions.

Analysis of the APE1 cleavage reaction was conducted on the *NEIL3* PQS in the dsDNA or G4 contexts with four- or five-track sequences (Figure 8A) by following the time dependency from 0−60 min by PAGE (Figure 8B). For the case with the AP analogue F at position 16 in the dsDNA context with four or five tracks, the time-course profiles were similar between the two sequences and reached high yields (Figure 8C). In contrast, the APE1-dependent strand cleavage yield for the G4 context with F at the loop produced poor cleavage yields even at long reaction times (Figure 8C). Next, time-dependent APE1 cleavage reactions were conducted with F at position 23 (i.e., a core position) to find that, in the dsDNA context, the yields were similar, as expected, while in the G4 context, the yield showed dependency on whether four or five G runs were present (Figure 8D). When four G tracks were present in the G4 context, the structure poorly forms on the basis of T_m analysis (Figure 7), allowing APE1-mediated cleavage to occur to some extent (Figure 8D, red squares). In contrast, with five G tracks present, the G4 is stable on the basis of T_m analysis, and the APE1 cleavage yield did not increase significantly above the background (Figure 8D, black crosses).

The reactions were then analyzed for the yield of strand scission at 10 min to make quantitative comparisons (Figure 8E). In the duplex context after 10 min, APE1 cleaved >50% of the reactant, while in the G4 context, product yields were near the background (<3%) with the exception of the most poorly formed G4 with F at a core position in the four-track *NEIL3* sequence. The presence of the fifth G track in the natural *NEIL3* sequence allows strong G4 folding to occur with a core F and prevents APE1-mediated cleavage of the modification. These data support the claim from Scheme 1E that APE1 activity is highly attenuated on substrates in the loops of stable G4 folds; further, the results in their entirety are consistent with prior studies regarding poor cleavage by APE1 of substrates in noncanonical contexts.[49,72] The final point is whether APE1 binds G4 folds, and this has been documented in prior studies.[49] Thus, binding of APE1 to an AP in the loop of a G4 stalls the catalytic function of this enzyme, allowing it to function as a trans-activator[73] of transcription (Scheme 1E). At present, we believe that APE1 interactions with HIF-1α and/or AP-1 are the likely protein interaction partners that lead to gene induction;[18] however, further studies are needed to complete our understanding.

Herein, the studies describe a plausible pathway by which the *NEIL3* DNA repair gene can be activated under oxidative or inflammatory stress conditions via oxidation of a G-rich promoter element followed by BER-initiated transcriptional activation (Scheme 1). The mechanistic proposal is supported by in vitro and in cellulo studies (Figures 3−8). The interplay of DNA repair of oxidatively modified DNA bases leading to gene activation has been previously documented,[15−17,19,20] and

DOI: 10.1021/jacs.9b01847
J. Am. Chem. Soc. 2019, 141, 11036−11049

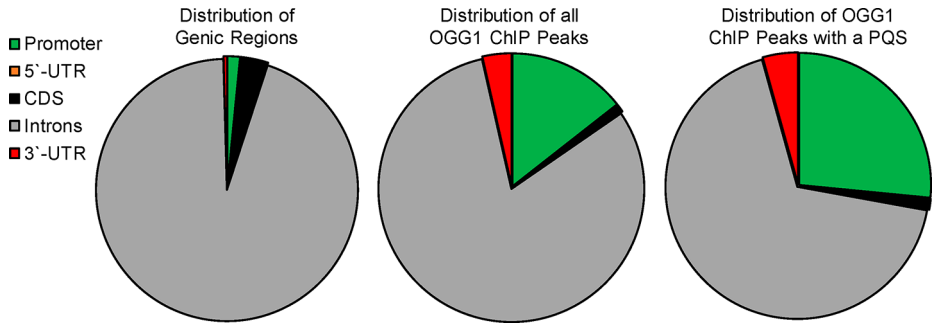

Figure 9. Additional analysis of published OGG1 ChIP-Seq data to find the distribution of PQSs in genic regions of oxidatively stressed HEK293 cells.[40] The three charts show (left) the relative distribution of genomic regions of interest, on a per nucleotide basis, obtained from the UCSC genome browser, (center) the relative distribution for all OGG1 ChIP-Seq peaks identified, and (right) the relative distribution of the peaks containing a PQS. The PQS-containing peaks represent ~10% of all peaks of OGG1 enrichment. It is noteworthy that the present analysis of the published results provided different absolute values for the number of enrichment peaks but the overall relative distribution and conclusions from the results remain the same as previously reported.[40]

the present studies are fully consistent with these findings. In contrast to cells experiencing oxidative or inflammatory stress, quiescent cells were found to stimulate *NEIL3* expression via the Ras-dependent ERK-MAP kinase pathway.[74] Whether overlap between the two pathways occurs is not currently known.

The findings from our work and others suggest that oxidative modification of G to OG in certain gene promoter contexts can function as an epigenetic-like DNA modification for gene regulation under stress conditions.[10−13] Importantly, we found for the first time that synthetic installation of OG into a promoter PQS mimicked the change in expression levels seen with oxidative stress induced by TNFα. To date, some of the readers, writers, and erasers of OG have been identified. The writers have been assigned as diffusible oxidants or as a consequence of chromatin remodeling. The chromatin remodeler LSD1 is a flavin-dependent monooxygenase that demethylates H2K4me2 or H3K9me2 to yield H_2O_2 as a byproduct, and it was found to oxidize G to OG in the genome;[16] LSD2 may serve the same function.[75] Exploration for other OG writing mechanisms is ongoing. Independently and by two different methods, OG was sequenced in mammalian genomes and found to be enriched in the context of PQSs, and gene promoters harbored more OG than expected by chance.[76,77] These sequencing results are consistent with the favorability of writing OG in promoter regions and provide support for our hypothesis. Because OG and its enzymatic conversion to an AP occur upstream of the TSS in the promoter, these modifications to the DNA will not impact synthesis of the mRNA strand in a way that could be identified by RNA-Seq analysis.

The OG reader found so far is the glycosylase OGG1 that has been assigned a few different possible functions for regulation of gene expression. Boldogh, Ba, and co-workers have found that OGG1 can function as a transcriptional modulator via controlling transcription factor homing to promoter sequences.[15] In another possible pathway, Xodo and co-workers have proposed that OG in the context of the *KRAS* PQS enables recruitment of MAZ and hnRNP A1 to the G4 for gene activation with the assistance of OGG1 to return the sequence back to the native state.[20] In our proposal, OG is initially read and acted on by OGG1 to form an AP site, allowing the sequence to shift structures to a noncanonical G4 fold for presentation of the AP to the second reader protein APE1.[19] Binding of APE1 to the G4 occurs, but the catalytic function to cleave the AP is attenuated (Figure 8), allowing this protein to function as a trans activator of transcription. Tell and co-workers have also assigned a critical role for APE1 as a trans activator of transcription for the SIRT1 gene under oxidative stress conditions, and their proposal also invokes a non-B-form DNA structure in the proposal (i.e., hairpin).[17] These pathways offer exciting observations that OG has epigenetic-like potential, and more studies will allow a better understanding of the myriad consequences of this simple addition of an oxygen atom to G in directing cellular processes.

Identification of OGG1 and APE1 homing to promoter regions of the genome for gene activation can be determined by ChIP-Seq analysis. Successful ChIP-Seq experiments require ChIP-grade antibodies that are not commercially available. In our hands, the available OGG1 and APE1 antibodies failed to provide usable ChIP-Seq results. Bypass of this challenge is achievable by expressing Flag-tagged OGG1 or APE1 from a transfected plasmid followed by ChIP analysis with a Flag antibody. Such an experiment was successfully employed for OGG1, which demonstrated that HEK293 cells exposed to TNFα had OGG1 enriched in gene promoters.[40] Gene ontology analysis of the enriched peaks found the response to oxidative stress and cell redox homeostasis ontologies to be the two most overrepresented groups.[40] As for APE1, a targeted ChIP analysis found promoter-bound APE1 stimulated recruitment of RNA pol II for gene activation.[78]

We conducted an inspection of the Flag-OGG1 ChIP-Seq data to locate peaks of 4-fold or greater enrichment with a PQS. Comparison of the distribution of all OGG1 ChIP peaks to those with a PQS identified that those with the G-rich sequence were somewhat more favorably enriched in promoter regions, consistent with our proposal (Figure 9). In the PQS-containing peaks in gene promoters, the *NEIL3* gene was not identified, likely due to the low overall expression of this gene in HEK293 cells studied (Figure S6). This finding does not directly support *NEIL3* activation by the proposed pathway, but the overall findings from the additional analysis of the OGG1 ChIP-Seq studies suggest that promoter PQSs are sites of OGG1 binding during oxidative stress that can potentially lead to gene activation.

The role for oxidation in PQSs and G4 folds in the activation process are the least defined to date; however, a growing body of evidence supports G4 folds in gene regulation,[79] and recent sequencing data from mammalian

DOI: 10.1021/jacs.9b01847
J. Am. Chem. Soc. 2019, 141, 11036−11049

genomes for OG has identified that a significant fraction (25−37%) of oxidized sites occur in PQS contexts.[76,77] We recognize the complementary strand to the *NEIL3* PQS is a potential i-motif-forming sequence that could play a role in gene activation as well. The i-motif fold is composed of hemiprotonated $(C:C)^+$ base pairs that typically form under acidic conditions, and specific i-motif folds have been suggested to upregulate transcription.[80,81] The examples to date occur in sequences capable of folding under pH conditions near neutrality, similar to the cellular pH. The *NEIL3* i-motif was studied and found to fold only under low pH conditions (pH < 6; Figure S7). As a result of the low stability of this i-motif under biologically relevant conditions, folding for this sequence is not expected unless facilitated by proteins.[81]

The proposal of the G4 strand guiding the process is consistent with BER serving a dual function in the cell to remove modified bases from the genome and to activate transcription;[12,19,66] therefore, the strand with the modification will be targeted by the BER proteins. Oxidation of G in the PQS context rather than the potential i-motif context is highly favored thermodynamically, and it consistently occurs at a 5′-G in G-runs as determined by many laboratories.[59−61] From a relative perspective, a 5′-GG is ∼10 kcal/mol, a 5′-GGG is ∼16 kcal/mol, and a 5′-GGGG is ∼18 kcal/mol more reactive toward one-electron oxidation than a single G.[82] In the *NEIL3* PQS sequence, the complementary strand has 5′-GG runs; however, the 5′-GGGG runs in the G4 sequence remain ∼8 kcal/mol more reactive toward oxidation than the C-rich strand, resulting in exclusive oxidation of the G-rich strand. To reiterate, this is important because it focuses the BER proteins to the most G-rich strand for gene activation. These observations and arguments do not completely dismiss i-motif folds in the process, but they make a case against their role in the activation of the *NEIL3* gene under oxidative or inflammatory stress conditions.

It is critical for a cell to respond to the insults that occur during oxidative stress. The NEIL3 DNA glycosylase protein is a part of the DNA repair network, although its complete cellular function has been challenging to determine.[4,83] Studies suggest that NEIL3 expression is activated during the S phase of the cell cycle,[70] which is the cycle in which G4s appear to be most active for gene regulation.[71] The NEIL3 glycosylase expression and activity appears to be coupled to replication.[4,83] During replication it is important to ensure the DNA is devoid of any modifications that may interfere with DNA replication. The substrate scope for the NEIL3 protein includes the G oxidation products Sp and Gh in ssDNA or G4 DNA, although these modifications are poor substrates for NEIL3 in dsDNA and are better removed by NEIL1.[48,84−87] Furthermore, NEIL3 appears to function also in the initial stages of DNA strand cross-link repair involving adduct formation to AP sites in DNA.[88,89] Lastly, APE1 may also function in repair of bulky adducts in ssDNA contexts.[90] The key point is that G oxidation products and DNA strand cross-links increase under oxidative stress conditions, and therefore, upregulation of the *NEIL3* gene to repair these promutagenic lesions would be essential for a cell to combat stress and pass on a high-integrity genome to daughter cells.

CONCLUSIONS

Oxidative and inflammatory stress generate ROS and RNS capable of oxidatively modifying DNA that historically has been thought of as a deleterious process leading to mutations. Attention derived from chemical and biological studies has led us to realize that oxidative modification of DNA can also function in gene regulation.[15,17,19,20] The oxidation of G to OG in gene promoters for regulation of proinflammatory genes,[15] including *BCL2*,[16] *VEGF*,[18,19] *SIRT1*,[17] and *KRAS*,[20] has been demonstrated, thus relegating the OG heterocycle to a list of epigenetic-like regulatory modifications in DNA. In the current work, we provide experimental support for the hypothesis that the *NEIL3* DNA repair gene can be regulated via oxidative modification of a promoter G to OG (Scheme 1). The proposed activation pathway is consistent with many cell and animal model studies which have shown that *NEIL3* is induced under oxidative stress or inflammation, and OG is formed in the genome during the activation process.[8,21−23,25,26] The proposed pathway is initiated by G oxidation to OG in the PQS found at position −3 relative to the TSS in the coding strand of the promoter. The presence of OG focuses the BER process for initial release of OG by OGG1 to yield a duplex-destabilizing AP site, providing the drive for a structural shift to a G4 fold. This fold places the AP site in a large loop that APE1 binds but poorly cleaves, allowing this endonuclease to function as a trans activator of transcription by recruitment of activating transcription factors (Scheme 1).[17,91] The proposed mechanism is supported by in vitro and in cellulo studies harnessing chemical tools to study biology (Figures 3−8). Upregulated expression of the NEIL3 DNA repair protein during stress can be crucial for repair of lesions in DNA such as the hyperoxidation products Sp and Gh, DNA interstrand cross-links, or bulky DNA adducts.[48,84−86,88−90] Moreover, the observation that the *NEIL3* PQS is conserved in many different mammals (Figure 2B) suggests that this sequence and its sensitivity toward oxidation have been favorably selected as a redox epigenetic unit for gene regulation. Future steps to support the findings from these chemically defined plasmid-based systems will require moving to the genome scale and use of various OG-seq,[76] ChIP-seq, and RNA-seq methods before and after oxidative stress to follow the choreography of DNA oxidation resulting in OGG1 and APE1 activity in gene promoters.

ASSOCIATED CONTENT

Supporting Information

The Supporting Information is available free of charge on the ACS Publications website at DOI: 10.1021/jacs.9b01847.

Complete experimental details, PAGE images, HPLC chromatograms, CD spectra, and T_m plots (PDF)

AUTHOR INFORMATION

Corresponding Authors

*afleming@chem.utah.edu

*burrows@chem.utah.edu

ORCID

Aaron M. Fleming: 0000-0002-2000-0310

Cynthia J. Burrows: 0000-0001-7253-8529

Notes

The authors declare no competing financial interest.

ACKNOWLEDGMENTS

We are grateful to the National Cancer Institute for supporting this research project via Grant no. R01 CA090689. The DNA

strand synthesis and Sanger sequencing were provided by the University of Utah Health Sciences Core facilities that are supported in part by a National Cancer Institute Cancer Center Support Grant (P30 CA042014). The authors thank Yun Ding (University of Utah) for her assistance with the cell studies.

REFERENCES

(1) Dedon, P. C.; Tannenbaum, S. R. *Arch. Biochem. Biophys.* **2004**, *423*, 12−22.
(2) Wiseman, H.; Halliwell, B. *Biochem. J.* **1996**, *313*, 17−29.
(3) Cadet, J.; Wagner, J. R.; Shafirovich, V.; Geacintov, N. E. *Int. J. Radiat. Biol.* **2014**, *90*, 423−432.
(4) Fleming, A. M.; Burrows, C. J. *Free Radical Biol. Med.* **2017**, *107*, 35−52.
(5) Pfeifer, G.; Besaratinia, A. *Hum. Genet.* **2009**, *125*, 493−506.
(6) David, S. S.; O'Shea, V. L.; Kundu, S. *Nature* **2007**, *447*, 941−950.
(7) Steenken, S. *Chem. Rev.* **1989**, *89*, 503−520.
(8) Mangerich, A.; Knutson, C. G.; Parry, N. M.; Muthupalani, S.; Ye, W.; Prestwich, E.; Cui, L.; McFaline, J. L.; Mobley, M.; Ge, Z.; Taghizadeh, K.; Wishnok, J. S.; Wogan, G. N.; Fox, J. G.; Tannenbaum, S. R.; Dedon, P. C. *Proc. Natl. Acad. Sci. U. S. A.* **2012**, *109*, E1820−E1829.
(9) Wood, M. L.; Esteve, A.; Morningstar, M. L.; Kuziemko, G. M.; Essigmann, J. M. *Nucleic Acids Res.* **1992**, *20*, 6023−6032.
(10) Fleming, A. M.; Burrows, C. J. *DNA Repair* **2017**, *56*, 75−83.
(11) Wang, R.; Hao, W.; Pan, L.; Boldogh, I.; Ba, X. *Cell. Mol. Life Sci.* **2018**, *75*, 3741−3750.
(12) Antoniali, G.; Malfatti, M. C.; Tell, G. *DNA Repair* **2017**, *56*, 65−74.
(13) Seifermann, M.; Epe, B. *Free Radical Biol. Med.* **2017**, *107*, 258−265.
(14) Visnes, T.; Cazares-Korner, A.; Hao, W.; Wallner, O.; Masuyer, G.; Loseva, O.; Mortusewicz, O.; Wiita, E.; Sarno, A.; Manoilov, A.; Astorga-Wells, J.; Jemth, A. S.; Pan, L.; Sanjiv, K.; Karsten, S.; Gokturk, C.; Grube, M.; Homan, E. J.; Hanna, B. M. F.; Paulin, C. B. J.; Pham, T.; Rasti, A.; Berglund, U. W.; von Nicolai, C.; Benitez-Buelga, C.; Koolmeister, T.; Ivanic, D.; Iliev, P.; Scobie, M.; Krokan, H. E.; Baranczewski, P.; Artursson, P.; Altun, M.; Jensen, A. J.; Kalderen, C.; Ba, X.; Zubarev, R. A.; Stenmark, P.; Boldogh, I.; Helleday, T. *Science* **2018**, *362*, 834−839.
(15) Pan, L.; Zhu, B.; Hao, W.; Zeng, X.; Vlahopoulos, S. A.; Hazra, T. K.; Hegde, M. L.; Radak, Z.; Bacsi, A.; Brasier, A. R.; Ba, X.; Boldogh, I. *J. Biol. Chem.* **2016**, *291*, 25553−25566.
(16) Perillo, B.; Ombra, M. N.; Bertoni, A.; Cuozzo, C.; Sacchetti, S.; Sasso, A.; Chiariotti, L.; Malorni, A.; Abbondanza, C.; Avvedimento, E. V. *Science* **2008**, *319*, 202−206.
(17) Antoniali, G.; Lirussi, L.; D'Ambrosio, C.; Dal Piaz, F.; Vascotto, C.; Casarano, E.; Marasco, D.; Scaloni, A.; Fogolari, F.; Tell, G. *Mol. Biol. Cell* **2014**, *25*, 532−547.
(18) Pastukh, V.; Roberts, J. T.; Clark, D. W.; Bardwell, G. C.; Patel, M.; Al-Mehdi, A. B.; Borchert, G. M.; Gillespie, M. N. *Am. J. Physiol. Lung Cell Mol. Physiol.* **2015**, *309*, L1367−1375.
(19) Fleming, A. M.; Ding, Y.; Burrows, C. J. *Proc. Natl. Acad. Sci. U. S. A.* **2017**, *114*, 2604−2609.
(20) Cogoi, S.; Ferino, A.; Miglietta, G.; Pedersen, E. B.; Xodo, L. E. *Nucleic Acids Res.* **2018**, *46*, 661−676.
(21) Sejersted, Y.; Hildrestrand, G. A.; Kunke, D.; Rolseth, V.; Krokeide, S. Z.; Neurauter, C. G.; Suganthan, R.; Atneosen-Asegg, M.; Fleming, A. M.; Saugstad, O. D.; Burrows, C. J.; Luna, L.; Bjoras, M. *Proc. Natl. Acad. Sci. U. S. A.* **2011**, *108*, 18802−18807.
(22) Wang, J.; Wang, Q.; Watson, L. J.; Jones, S. P.; Epstein, P. N. *Am. J. Physiol. Heart Circ. Physiol.* **2011**, *301*, H2073−H2080.
(23) Olsen, M. B.; Hildrestrand, G. A.; Scheffler, K.; Vinge, L. E.; Alfsnes, K.; Palibrk, V.; Wang, J.; Neurauter, C. G.; Luna, L.; Johansen, J.; Ogaard, J. D. S.; Ohm, I. K.; Slupphaug, G.; Kusnierczyk, A.; Fiane, A. E.; Brorson, S. H.; Zhang, L.; Gullestad, L.; Louch, W. E.; Iversen, P. O.; Ostlie, I.; Klungland, A.; Christensen, G.; Sjaastad, I.; Saetrom, P.; Yndestad, A.; Aukrust, P.; Bjoras, M.; Finsen, A. V. *Cell Rep.* **2017**, *18*, 82−92.
(24) Obtułowicz, T.; Swoboda, M.; Speina, E.; Gackowski, D.; Rozalski, R.; Siomek, A.; Janik, J.; Janowska, B.; Cieśla, J. M.; Jawien, A.; Banaszkiewicz, Z.; Guz, J.; Dziaman, T.; Szpila, A.; Olinski, R.; Tudek, B. *Mutagenesis* **2010**, *25*, 463−471.
(25) Shinmura, K.; Kato, H.; Kawanishi, Y.; Igarashi, H.; Goto, M.; Tao, H.; Inoue, Y.; Nakamura, S.; Misawa, K.; Mineta, H.; Sugimura, H. *Oxid. Med. Cell. Longev.* **2016**, *2016*, 1546392.
(26) Rognlien, A. G.; Wollen, E. J.; Atneosen-Asegg, M.; Saugstad, O. D. *Pediatr. Res.* **2015**, *77*, 326−333.
(27) Sejersted, Y.; Aasland, A. L.; Bjoras, M.; Eide, L.; Saugstad, O. D. *Pediatr. Res.* **2009**, *66*, 533−538.
(28) Fleming, A. M.; Zhu, J.; Ding, Y.; Visser, J. A.; Zhu, J.; Burrows, C. J. *Biochemistry* **2018**, *57*, 991−1002.
(29) Gray, R. D.; Chaires, J. B. *Nucleic Acids Res.* **2008**, *36*, 4191−4203.
(30) Patel, D. J.; Phan, A. T.; Kuryavyi, V. *Nucleic Acids Res.* **2007**, *35*, 7429−7455.
(31) Mergny, J. L.; Sen, D. *Chem. Rev.* **2019**, *119*, 6290−6325, DOI: 10.1021/acs.chemrev.8b00629.
(32) Omaga, C. A.; Fleming, A. M.; Burrows, C. J. *Biochemistry* **2018**, *57*, 2958−2970.
(33) Fong, Y. W.; Cattoglio, C.; Tjian, R. *Mol. Cell* **2013**, *52*, 291−302.
(34) Redstone, S. C. J.; Fleming, A. M.; Burrows, C. J. *Chem. Res. Toxicol.* **2019**, *32*, 437−446.
(35) Fleming, A. M.; Burrows, C. J. *Chem. Res. Toxicol.* **2013**, *26*, 593−607.
(36) Chen, X.; Fleming, A. M.; Muller, J. G.; Burrows, C. J. *New J. Chem.* **2013**, *37*, 3440−3449.
(37) Riedl, J.; Fleming, A. M.; Burrows, C. J. *J. Am. Chem. Soc.* **2016**, *138*, 491−494.
(38) Klungland, A.; Rosewell, I.; Hollenbach, S.; Larsen, E.; Daly, G.; Epe, B.; Seeberg, E.; Lindahl, T.; Barnes, D. E. *Proc. Natl. Acad. Sci. U. S. A.* **1999**, *96*, 13300−13305.
(39) Fleming, A. M.; Zhu, J.; Ding, Y.; Burrows, C. J. *ACS Chem. Biol.* **2017**, *12*, 2417−2426.
(40) Hao, W.; Qi, T.; Pan, L.; Wang, R.; Zhu, B.; Aguilera-Aguirre, L.; Radak, Z.; Hazra, T. K.; Vlahopoulos, S. A.; Bacsi, A.; Brasier, A. R.; Ba, X.; Boldogh, I. *Redox Biol.* **2018**, *18*, 43−53.
(41) Afgan, E.; Baker, D.; Batut, B.; van den Beek, M.; Bouvier, D.; Čech, M.; Chilton, J.; Clements, D.; Coraor, N.; Grüning, B. A.; Guerler, A.; Hillman-Jackson, J.; Hiltemann, S.; Jalili, V.; Rasche, H.; Soranzo, N.; Goecks, J.; Taylor, J.; Nekrutenko, A.; Blankenberg, D. *Nucleic Acids Res.* **2018**, *46*, W537−W544.
(42) Langmead, B.; Trapnell, C.; Pop, M.; Salzberg, S. L. *Genome Biol.* **2009**, *10*, R25.
(43) Zhang, Y.; Liu, T.; Meyer, C. A.; Eeckhoute, J. r. m.; Johnson, D. S.; Bernstein, B. E.; Nusbaum, C.; Myers, R. M.; Brown, M.; Li, W.; Liu, X. S. *Genome biology* **2008**, *9*, R137.
(44) Huppert, J. L.; Balasubramanian, S. *Nucleic Acids Res.* **2005**, *33*, 2908−2916.
(45) Huang, W.; Loganantharaj, R.; Schroeder, B.; Fargo, D.; Li, L. *Bioinformatics* **2013**, *29*, 3097−3099.
(46) Khaper, N.; Bryan, S.; Dhingra, S.; Singal, R.; Bajaj, A.; Pathak, C. M.; Singal, P. K. *Antioxid. Redox Signaling* **2010**, *13*, 1033−1049.
(47) Crean, C.; Geacintov, N. E.; Shafirovich, V. *Angew. Chem., Int. Ed.* **2005**, *44*, 5057−5060.
(48) Fleming, A. M.; Zhou, J.; Wallace, S. S.; Burrows, C. J. *ACS Cent. Sci.* **2015**, *1*, 226−233.
(49) Broxson, C.; Hayner, J. N.; Beckett, J.; Bloom, L. B.; Tornaletti, S. *Nucleic Acids Res.* **2014**, *42*, 7708−7719.
(50) Cadet, J.; Douki, T.; Gasparutto, D.; Ravanat, J.-L. *Mutat. Res., Fundam. Mol. Mech. Mutagen.* **2003**, *531*, 5−23.
(51) Rokhlenko, Y.; Geacintov, N. E.; Shafirovich, V. *J. Am. Chem. Soc.* **2012**, *134*, 4955−4962.

DOI: 10.1021/jacs.9b01847
J. Am. Chem. Soc. 2019, 141, 11036−11049

(52) Luo, W.; Muller, J. G.; Rachlin, E. M.; Burrows, C. J. *Org. Lett.* **2000**, *2*, 613−616.
(53) Luo, W.; Muller, J. G.; Rachlin, E. M.; Burrows, C. J. *Chem. Res. Toxicol.* **2001**, *14*, 927−938.
(54) Matter, B.; Malejka-Giganti, D.; Csallany, A. S.; Tretyakova, N. *Nucleic Acids Res.* **2006**, *34*, 5449−5460.
(55) Hailer, M. K.; Slade, P. G.; Martin, B. D.; Sugden, K. D. *Chem. Res. Toxicol.* **2005**, *18*, 1378−1383.
(56) Zhu, J.; Fleming, A. M.; Burrows, C. J. *ACS Chem. Biol.* **2018**, *13*, 2577−2584.
(57) Fleming, A. M.; Alshykhly, O.; Zhu, J.; Muller, J. G.; Burrows, C. J. *Chem. Res. Toxicol.* **2015**, *28*, 1292−1300.
(58) Muller, J. G.; Duarte, V.; Hickerson, R. P.; Burrows, C. J. *Nucleic Acids Res.* **1998**, *26*, 2247−2249.
(59) Delaney, S.; Barton, J. K. *J. Org. Chem.* **2003**, *68*, 6475−6483.
(60) Saito, I.; Takayama, M.; Sugiyama, H.; Nakatani, K.; Tsuchida, A.; Yamamoto, M. *J. Am. Chem. Soc.* **1995**, *117*, 6406−6407.
(61) Schuster, G. B. *Acc. Chem. Res.* **2000**, *33*, 253−260.
(62) Xu, X.; Muller, J. G.; Ye, Y.; Burrows, C. J. *J. Am. Chem. Soc.* **2008**, *130*, 703−709.
(63) Cadet, J.; Berger, M.; Buchko, G. W.; Joshi, P. C.; Raoul, S.; Ravanat, J.-L. *J. Am. Chem. Soc.* **1994**, *116*, 7403−7404.
(64) Steenken, S.; Jovanovic, S. V.; Bietti, M.; Bernhard, K. *J. Am. Chem. Soc.* **2000**, *122*, 2373−2374.
(65) Alshykhly, O. R.; Fleming, A. M.; Burrows, C. J. *J. Org. Chem.* **2015**, *80*, 6996−7007.
(66) Allgayer, J.; Kitsera, N.; Bartelt, S.; Epe, B.; Khobta, A. *Nucleic Acids Res.* **2016**, *44*, 7267−7280.
(67) Schermerhorn, K. M.; Delaney, S. *Biochemistry* **2013**, *52*, 7669−7677.
(68) Zorzan, E.; Elgendy, R.; Giantin, M.; Dacasto, M.; Sissi, C. *Sci. Rep.* **2018**, *8*, 17107.
(69) Pagano, A.; Iaccarino, N.; Abdelhamid, M. A. S.; Brancaccio, D.; Garzarella, E. U.; Di Porzio, A.; Novellino, E.; Waller, Z. A. E.; Pagano, B.; Amato, J.; Randazzo, A. *Front. Chem.* **2018**, *6*, 281.
(70) Zhou, J.; Chan, J.; Lambele, M.; Yusufzai, T.; Stumpff, J.; Opresko, P. L.; Thali, M.; Wallace, S. S. *Cell Rep.* **2017**, *20*, 2044−2056.
(71) Biffi, G.; Tannahill, D.; McCafferty, J.; Balasubramanian, S. *Nat. Chem.* **2013**, *5*, 182−186.
(72) Burra, S.; Marasco, D.; Malfatti, M. C.; Antoniali, G.; Virgilio, A.; Esposito, V.; Demple, B.; Galeone, A.; Tell, G. *DNA Repair* **2019**, *73*, 129−143.
(73) Bhakat, K. K.; Mantha, A. K.; Mitra, S. *Antioxid. Redox Signaling* **2009**, *11*, 621−638.
(74) Neurauter, C. G.; Luna, L.; Bjoras, M. *DNA Repair* **2012**, *11*, 401−409.
(75) van Essen, D.; Zhu, Y.; Saccani, S. *Mol. Cell* **2010**, *39*, 750−760.
(76) Ding, Y.; Fleming, A. M.; Burrows, C. J. *J. Am. Chem. Soc.* **2017**, *139*, 2569−2572.
(77) Amente, S.; Di Palo, G.; Scala, G.; Castrignanò, T.; Gorini, F.; Cocozza, S.; Moresano, A.; Pucci, P.; Ma, B.; Stepanov, I.; Lania, L.; Pelicci, P. G.; Dellino, G. I.; Majello, B. *Nucleic Acids Res.* **2019**, *47*, 221−236.
(78) Sengupta, S.; Mantha, A. K.; Mitra, S.; Bhakat, K. K. *Oncogene* **2011**, *30*, 482−493.
(79) Hansel-Hertsch, R.; Beraldi, D.; Lensing, S. V.; Marsico, G.; Zyner, K.; Parry, A.; Di Antonio, M.; Pike, J.; Kimura, H.; Narita, M.; Tannahill, D.; Balasubramanian, S. *Nat. Genet.* **2016**, *48*, 1267−1272.
(80) Abou Assi, H.; Garavis, M.; Gonzalez, C.; Damha, M. J. *Nucleic Acids Res.* **2018**, *46*, 8038−8056.
(81) Kang, H. J.; Kendrick, S.; Hecht, S. M.; Hurley, L. H. *J. Am. Chem. Soc.* **2014**, *136*, 4172−4185.
(82) Sugiyama, H.; Saito, I. *J. Am. Chem. Soc.* **1996**, *118*, 7063−7068.
(83) Liu, M.; Doublie, S.; Wallace, S. S. *Mutat. Res., Fundam. Mol. Mech. Mutagen.* **2013**, *743*−*744*, 4−11.
(84) Liu, M.; Bandaru, V.; Bond, J. P.; Jaruga, P.; Zhao, X.; Christov, P. P.; Burrows, C. J.; Rizzo, C. J.; Dizdaroglu, M.; Wallace, S. S. *Proc. Natl. Acad. Sci. U. S. A.* **2010**, *107*, 4925−4930.
(85) Zhou, J.; Fleming, A. M.; Averill, A. M.; Burrows, C. J.; Wallace, S. S. *Nucleic Acids Res.* **2015**, *43*, 4039−4054.
(86) Zhou, J.; Liu, M.; Fleming, A. M.; Burrows, C. J.; Wallace, S. S. *J. Biol. Chem.* **2013**, *288*, 27263−27272.
(87) Krishnamurthy, N.; Zhao, X.; Burrows, C. J.; David, S. S. *Biochemistry* **2008**, *47*, 7137−7146.
(88) Semlow, D. R.; Zhang, J.; Budzowska, M.; Drohat, A. C.; Walter, J. C. *Cell* **2016**, *167*, 498−511.
(89) Yang, Z.; Nejad, M. I.; Varela, J. G.; Price, N. E.; Wang, Y.; Gates, K. S. *DNA Repair* **2017**, *52*, 1−11.
(90) Minko, I. G.; Christov, P. P.; Li, L.; Stone, M. P.; McCullough, A. K.; Lloyd, R. S. *DNA Repair* **2019**, *73*, 49−54.
(91) Tell, G.; Quadrifoglio, F.; Tiribelli, C.; Kelley, M. R. *Antioxid. Redox Signaling* **2009**, *11*, 601−620.

DOI: 10.1021/jacs.9b01847
J. Am. Chem. Soc. 2019, 141, 11036−11049